NACA

RESEARCH MEMORANDUM

LOW-SPEED INVESTIGATION OF DEFLECTABLE WING-TIP AILERONS ON AN UNTAPERED 45° SWEPTBACK SEMISPAN WING WITH AND WITHOUT AN END PLATE

By Jack Fischel and James M. Watson

Langley Aeronautical Laboratory
Langley Air Force Base, Va.

NATIONAL ADVISORY COMMITTEE
FOR AERONAUTICS

WASHINGTON

December 14, 1949

NATIONAL ADVISORY COMMITTEE FOR AERONAUTICS

RESEARCH MEMORANDUM

LOW-SPEED INVESTIGATION OF DEFLECTABLE WING-TIP AILERONS ON AN UNTAPERED 45° SWEPTBACK SEMISPAN WING WITH AND WITHOUT AN END PLATE

By Jack Fischel and James M. Watson

SUMMARY

A low-speed wind-tunnel investigation to determine the characteristics of deflectable wing-tip ailerons on an untapered 45° sweptback semispan wing was made in the Langley 300 MPH 7- by 10-foot tunnel. The ailerons investigated had triangular and parallelogram plan forms with a maximum chord of 0.625 wing chord and a flat-plate profile. These ailerons were tested on the plain wing and on the wing with a rectangular end plate (to simulate a vertical fin) mounted inboard of the ailerons.

The results of the investigation indicated that the plan form of the aileron had little effect on the lift, drag, and pitching-moment characteristics of the wing. The addition of the end plate, however, increased the wing lift-curve slope and the drag, but decreased the maximum lift and the lift-drag ratio of the wing.

Aileron plan form generally had little effect on the values of rolling-moment coefficient produced by aileron deflection; however, the ailerons were more effective on the plain wing than on the wing with end plate. The ailerons should provide adequate lateral control over the entire angle-of-attack range investigated. The yawing moments resulting from aileron deflection were generally adverse - particularly at large angles of attack and aileron deflections.

INTRODUCTION

The NACA is currently investigating various devices for use in providing adequate lateral control on transonic and supersonic wing configurations. The deflectable wing-tip aileron is one of the control devices being investigated. This aileron consists of the entire tip of

the wing and is deflected about a spanwise hinge axis approximately normal to the plane of symmetry to produce rolling moment. The ailerons are, of course, deflected oppositely on each semispan of a complete wing in a manner similar to conventional ailerons.

Previous investigations of wing-tip ailerons deflected from a free-floating position have been made on more conventional (unswept) wings, and have shown adequate lateral control obtainable with this type of aileron (references 1 to 4). The results of a preliminary investigation of a triangular wing-tip aileron deflected 30° at an angle of attack of 0° on a 42° sweptback wing showed that this control surface provided large rolling moments at both subsonic and transonic speeds (reference 5). In addition, data obtained in an investigation of various extensible-type wing-tip ailerons at several small deflections on a 45° sweptback wing showed that a deflectable wing-tip aileron offered promise of providing large rolling moments on a sweptback wing (reference 6).

The present investigation on an untapered 45° sweptback semispan wing was performed in the Langley 300 MPH 7- by 10-foot tunnel in order to determine the lateral control characteristics of deflectable-type wing-tip ailerons on a sweptback wing. A parallelogram- and a triangular-plan-form wing-tip aileron having flat-plate profiles and equal areas were investigated on the wing model through a large wing-angle-of-attack range and at aileron deflections up to 30°. These ailerons were investigated with and without a large end plate (simulating a vertical fin) mounted on the wing inboard of the aileron in order to determine the effect of the end plate on both the plain-wing and aileron characteristics.

SYMBOLS

Inasmuch as the span of the wing equipped with the parallelogram and triangular ailerons differed appreciably (fig. 1), all data presented are based on the dimensions of each complete-wing configuration.

The forces and moments measured on the wings are presented about the wind axes, which, for the conditions of these tests (zero yaw), correspond to the stability axes. The X-axis is in the plane of symmetry of the models and is parallel to the tunnel free-stream air flow. The Z-axis is in the plane of symmetry of the models and is perpendicular to the X-axis. The Y-axis is mutually perpendicular to the X-axis and Z-axis. All three axes intersect at the intersection of the chord plane and the 25-percent station of the mean aerodynamic chord at the root of the models (fig. 1).

The symbols used in the presentation of results are as follows:

C_L lift coefficient (twice lift of semispan model/qS)

C_D drag coefficient (D/qS)

C_m pitching-moment coefficient ($M/qS\bar{c}$)

C_l rolling-moment coefficient (L/qSb)

C_n yawing-moment coefficient (N/qSb)

pb/2V wing-tip helix angle, radians

C_{l_p} damping-in-roll coefficient; that is, rate of change of rolling-moment coefficient with wing-tip helix angle $\left(\partial C_l / \partial\left(\frac{pb}{2V}\right)\right)$

$\bar{c}$ wing mean aerodynamic chord $\left(\frac{2}{S}\int_0^{b/2} c^2 dy\right)$
(wing with parallelogram-plan-form aileron, 3.42 ft; wing with triangular-plan-form aileron, 3.36 ft)

c local wing chord, feet

b twice span of each semispan model, including aileron
(wing with parallelogram-plan-form aileron, 6.28 ft; wing with triangular-plan-form aileron, 6.97 ft)

y lateral distance from plane of symmetry, feet

S twice area of each semispan model, including aileron
(21.02 sq ft)

D twice drag of semispan models, pounds

M twice pitching moment of semispan model about Y-axis, foot-pounds

L rolling moment, resulting from aileron deflection, about X-axis, foot-pounds

N yawing moment, resulting from aileron deflection, about Z-axis, foot-pounds

q free-stream dynamic pressure, pounds per square foot $\left(\frac{1}{2}\rho V^2\right)$

V free-stream velocity, feet per second

ρ mass density of air, slugs per cubic foot

α angle of attack with respect to chord plane at root of models, degrees

δ_a aileron deflection, measured between wing chord plane and aileron chord plane (positive when trailing edge is down), degrees

δ_{a_t} total aileron deflection

A wing aspect ratio (b^2/S)
(wing with parallelogram-plan-form aileron, 1.87; wing with triangular-plan-form aileron, 2.31)

$C_{l_{\delta_a}}$ rate of change of rolling-moment coefficient with aileron deflection $\left(\partial C_l/\partial \delta_a\right)$

CORRECTIONS

The angle-of-attack and the drag data have been corrected for jet-boundary (induced-upwash) effects according to the methods outlined in reference 7. Blockage corrections were applied to the test data by the methods of reference 8.

Reflection-plane corrections were not applied to the rolling-moment and yawing-moment data because available correction data did not apply to the configurations of this investigation. However, by extrapolation of the correction data of reference 9, it is estimated that the values of C_l presented herein were approximately 10 percent too high for both wing-aileron configurations. In addition, the yawing moments, if corrected, would be generally more adverse than the data show.

MODEL AND APPARATUS

The right semispan wing model was mounted vertically in the Langley 300 MPH 7- by 10-foot tunnel with the root chord of the model adjacent

to the ceiling (fig. 2), the ceiling thereby acting as a reflection plane. The wing, exclusive of ailerons, was constructed of steel and mahogany to the plan-form dimensions shown in figure 1. The wing had NACA 64A010 airfoil sections normal to the wing leading edge and had neither twist nor dihedral. The wing tip was a body of revolution.

A vertical end plate which roughly approximated a vertical tail surface was mounted on the main part of the wing, inboard of the wing-tip body of revolution, for a portion of the investigation. This end plate was a $\frac{1}{2}$-inch-thick sheet of plywood with rounded edges and was cut to the plan-form dimensions and mounted on the wing as shown in figure 1.

Two plan forms of wing-tip ailerons were used in the present investigation; one aileron had a parallelogram plan form, and the other a triangular plan form. Both ailerons had root chords of 0.625c and equal areas (fig. 1). The ailerons were constructed of $\frac{1}{4}$-inch-sheet duralumin with a rounded leading edge and a 12° beveled trailing edge along the entire span of each aileron. The trailing edges of both ailerons were swept back 45°. The ailerons were deflected about a spanwise axis passing through the 0.5-tip-chord station of the wing and the 0.5-root-chord station of the aileron.

Although the ailerons investigated did not have a conventional airfoil section, as would probably be the case in a practical application, the ailerons are believed to simulate an actual airplane arrangement sufficiently well to supply representative data.

TESTS

All tests of the 45° sweptback wing with the parallelogram- and triangular-plan-form wing-tip ailerons were performed in the Langley 300 MPH 7- by 10-foot tunnel at a dynamic pressure of approximately 50.5 pounds per square foot, which corresponds to a Mach number of 0.19 and a Reynolds number of about 4.4×10^6 based on the wing mean aerodynamic chord.

The aerodynamic characteristics in pitch were determined for the wing-aileron configurations with and without the end plate through an angle-of-attack range from positive to negative wing stall. The lateral control characteristics of each wing-aileron configuration (with and without the end plate) were also determined through a similar angle-of-attack range at various aileron deflections between 0° and approximately 30°.

DISCUSSION

Aerodynamic Characteristics in Pitch

The lift, drag, and pitching-moment coefficients for the plain wing and for the wing with the end plate are presented in figures 3 and 4, respectively.

The data of figures 3 and 4 show that a change in aileron plan form had little or no effect on the aerodynamic characteristics of the plain wing or the wing with the end plate. For all configurations investigated, the wing aerodynamic center was between about $0.23\bar{c}$ and $0.25\bar{c}$ at the low lift coefficients, and stable pitching-moment characteristics were exhibited at the wing stall.

The effect on the lift characteristics of adding the end plate to the wing was to increase the lift-curve slope from 0.040 to 0.046 and to decrease the maximum lift coefficient by approximately 0.23. (Compare figs. 3 and 4.) Although the effect of an end plate in increasing the wing lift-curve slope has been found previously on unswept wings (reference 10) and results from an increase in the effective aspect ratio of the wing, the unswept wings also showed an increase in maximum lift coefficient when the end plate was added (references 10 and 11). The aforementioned values of lift-curve slope obtained on the wing configurations reported herein (0.040 on the plain wing and 0.046 on the wing with end plate) correspond to effective aspect ratios of about 1.8 and 2.3, according to the charts of reference 12. It is of interest to note that, although the plain wing with the triangular-plan-form aileron had a geometric aspect ratio of 2.31, its effective aspect ratio was less (about 1.8). The reason for this phenomenon is unknown at present.

The addition of the end plate to the wing also produced an increase in the values of drag coefficient and an appreciable decrease in the values of the lift-drag ratio over the entire lift-coefficient range (figs. 3 and 4). This increase in drag coefficient was fairly small and constant at low values of lift coefficient (up to about 0.6 lift coefficient) and became fairly large at high values of lift coefficient. The break in the curve of pitching-moment coefficient plotted against lift coefficient and the decrease in the slope of the lift curve of the wing with end plate for values of C_L above 0.6 indicate some form of separation or adverse flow effects at the wing end-plate juncture. This in all probability causes the much larger values of drag coefficient for the wing with end plate. Reference 11, however, indicates that the drag coefficient of unswept wings is less at moderate and large lift coefficients with an end plate installed than without one.

The pitching-moment data obtained on the wing with and without the end plate were about the same, except that the wing with the end plate was slightly less stable than the plain wing.

Lateral Control Characteristics

The rolling-moment and yawing-moment data obtained through the angle-of-attack range from tests of the 45° sweptback wing at positive deflections of the wing-tip ailerons are presented in figures 5 to 8. In order to show the variation of rolling-moment coefficient with aileron deflection, the rolling-moment data of figures 5 to 8 were cross-plotted against aileron deflection as shown in figures 9 and 10. Inasmuch as all wing-aileron configurations investigated were symmetrical and had symmetrical profiles (although the end plate was asymmetrically placed on the wing), the rolling-moment data obtained at positive aileron deflections and negative angles of attack (figs. 5 to 8) were cross-plotted with opposite signs in figures 9 and 10 to provide data at negative aileron deflections and positive angles of attack.

Effect of aileron plan form.- A comparison of the data obtained with the triangular and parallelogram wing-tip ailerons reveals an inconsistent effect of aileron plan form on the rolling moments over the angle-of-attack range (figs. 5 to 8). The rolling-moment data presented in figures 5 to 10 also show that a serious reduction of rolling moment occurred for positive aileron deflections at the higher positive angles of attack, and in some cases, the aileron effectiveness reversed. This loss in effectiveness and the aileron reversal probably result from the stalling of the aileron at large deflections and wing angles of attack. Because wing stall angle generally increases with angle of sweepback, particularly with sharp leading edges, the triangular-plan-form aileron exhibited less tendency toward aileron reversal than the parallelogram-plan-form aileron. Similar effects of a large reduction and reversal of aileron effectiveness at large positive values of α and δ_a were not exhibited by the data of references 1 to 4 because the ailerons of the reference investigations were "free floating" - which enabled them to assume low incidences in the neutral condition - and also had conventional airfoil profiles, so that the ailerons did not stall when deflected to moderate deflections.

A comparison of the values of the slope of rolling-moment coefficient against aileron deflection $C_{l_{\delta_a}}$ at $\alpha = 0^\circ$ for the four wing-aileron configurations is shown in the following table:

Aileron plan form	$C_{l_{\delta_a}}$	
	Plain wing	Wing with end plate
Triangular	0.00072	0.00061
Parallelogram	.00072	.00047

Although the values of $C_{l_{\delta_a}}$ for the two aileron plan forms on the wing with end plate differed appreciably at $\alpha = 0^\circ$, aileron plan form generally had little effect on the rolling moments of either the plain wing or the wing with end plate over most of the angle-of-attack range. In addition, all aileron configurations exhibited larger values of $C_{l_{\delta_a}}$ at $\alpha = 5^\circ$ and 10° than at $\alpha = 0^\circ$ (figs. 9 and 10).

The yawing-moment data shown in figures 5 to 8 exhibit little or no consistent effect of aileron plan form. Although the yawing-moment data have not been cross-plotted against aileron deflection (as were the rolling-moment data), the values of C_n for positive angles of attack and negative aileron deflections would retain the same signs and values as shown in figures 5 to 8 for negative values of α and positive values of δ_a. Analysis of these data in conjunction with the rolling-moment data of figures 9 and 10 shows that the yawing moments were generally adverse and became more adverse with increase in angles of attack and aileron deflection. At the higher angles of attack, the adverse C_n/C_l ratio amounted to as much as 1.5 for all aileron configurations.

Effect of end plate.- The data obtained on the wing with end plate (figs. 7 and 8) generally showed a decrease in the rolling moments obtained through most of the angle-of-attack range and over the aileron-deflection range, compared with the rolling moments produced on the plain wing (figs. 5 and 6). This effect probably results from the fact that the end plate reduces any "carry-over" of loading from the aileron to the wing and vice versa, and causes the aileron to act essentially as an independent semispan wing in the presence of the end plate. As an independent wing, the aileron, because of its low aspect ratio and large sweep, produces small increments of lift - hence, small values of rolling moment for given deflections - and is less effective than the

aileron without the end plate, which evidently benefits from the "carry-over" between wing and aileron. Figures 5 to 8 show that the ailerons in the presence of the end plate maintained their effectiveness to higher positive angles of attack (at positive aileron deflections) before exhibiting trends toward reduction of C_l than did the ailerons on the plain wing. This favorable effect of the end plate may result from the elimination of any mutual adverse effects between the wing and aileron resulting from the wing-aileron juncture, or from the elimination of upflow around the wing tip.

The yawing moments obtained on the wing with end plate were usually less adverse than those obtained on the plain wing over the entire angle-of-attack range, particularly at low values of angle of attack.

In order to verify that the wing-tip aileron acts as an independent semispan wing in the presence of the end plate - which, if true, would allow the estimation of the aileron rolling effectiveness for such configurations fairly simply - calculations were made of the rolling moments contributed by the ailerons on the wing with the end plate. The estimated values of rolling-moment coefficient were calculated by the relationship

$$C_l = \frac{(\text{Lift of wing-tip aileron})(\text{Moment arm of wing-tip aileron})}{qSb}$$

for various aileron deflections at $\alpha = 0^\circ$. The lift of the triangular aileron used in the preceding equation was computed from the data of reference 13 and the lift of the parallelogram aileron was computed from the data of reference 14. The estimated values of C_l thereby calculated are compared with the test values of C_l in figure 11. In addition, the estimated and test values of C_l for the wing-tip aileron on the wing of reference 5 (at a Mach number of 0.5) are shown in figure 11. Estimated values of C_l at values of α other than 0° were also computed for the present ailerons, but were limited by the lack of aileron lift data at large angles of incidence - where stalled-flow conditions exist over the aileron - and are not compared herein with the test values of C_l. The excellent agreement obtained between all estimated and test values of C_l indicate that the aileron effectiveness of wing-tip ailerons mounted outboard of an end plate may be computed by this procedure. Because of the greater effectiveness of the ailerons without the end plate, the aforementioned method would provide conservative estimates of the aileron effectiveness for such wing configurations.

Rolling performance.– In order to illustrate the rolling effectiveness of the ailerons investigated, values of the wing-tip helix angle $pb/2V$ were calculated for each aileron configuration from the data of figures 5 to 8 and the curves of figures 12 and 13 and are presented in figures 14 to 16. The three aileron linkage systems used in these calculations provided differentials (at maximum aileron deflection) of 1:1 (equal up and down deflections), approximately 2:1, and approximately 3:1. (See fig. 12.) The estimated values of $pb/2V$ were obtained from the relationship $\frac{pb}{2V} = \frac{C_l}{C_{l_p}}$. The values of C_{l_p} used for determining the values of $pb/2V$ were obtained from the expression $C_{l_p} = \left(C_{l_p}\right)_{C_L=0} \frac{\left(C_{L_\alpha}\right)_{C_L}}{\left(C_{L_\alpha}\right)_{C_L=0}}$ presented as method 1 in reference 15 and are shown in figure 13. The values of $\left(C_{l_p}\right)_{C_L=0}$ used in the foregoing equation were −0.17 for the wing with the parallelogram-plan-form aileron and −0.21 for the wing with the triangular-plan-form aileron and were obtained from reference 12. Because the magnitude of the effects of the end plate on C_{l_p} are not known, similar values of $\left(C_{l_p}\right)_{C_L=0}$ were used for the plain wing and the wing with end plate; however, because of its larger value of lift-curve slope, the wing with end plate is expected to have larger values of C_{l_p} than those shown in figure 13, and unpublished damping-in-roll data corroborate this belief. The values of C_l used in calculating $pb/2V$ are the values thought to exist during steady rolling; that is, the difference in angle of attack of the two wing semispans due to rolling has been taken into account. No corrections were made to the values of $pb/2V$ to correct for the effects of adverse yaw or wing twist on the rolling effectiveness of these ailerons on an airplane. In addition, it should be remembered (as previously discussed) that reflection-plane corrections were not applied to the rolling-moment data.

The data of figures 14 to 16 show that the required value of the helix angle of 0.09 specified in reference 16 may generally be obtained with approximately 27° total deflection of the triangular or parallogram ailerons on the plain wing, regardless of the aileron differential employed; about 8° more total aileron deflection would generally be required from the corresponding ailerons on the wing with end plate. Although, as previously discussed, aileron plan form had little effect on the values of C_l obtained, the larger values of C_{l_p} used for the

wing with the triangular aileron accounts for the larger values of $pb/2V$ usually obtained with the parallelogram ailerons. In general, because of the differences in the variation of the values of C_{l_p} with α for the plain wing and the wing with end plate, the rolling effectiveness of the ailerons on the wing with end plate exhibited large increases with increase in α as contrasted to the smaller increases in rolling effectiveness with increase in α (up to $\alpha = 10^\circ$) exhibited by the ailerons on the plain wing. As a result of these trends, the ailerons on the wing with end plate produced larger values of $pb/2V$ at large values of α than did the ailerons on the plain wing; however, if the true variation of C_{l_p} with α for the wing with end plate were known, the results may differ somewhat from those shown by the present data. The data of figures 14 to 16 also show that the aileron differential generally had a negligible effect on the rolling performance of any wing–aileron configuration, except possibly at very large angles of attack, for which an increased rolling effectiveness is usually exhibited by employing the 2:1 or 3:1 differential as compared with the 1:1 differential.

As previously discussed, the effects of adverse aileron yaw on the estimated rolling–performance characteristics shown in figures 14 to 16 have not been considered in the calculations. These adverse yawing moments would tend to reduce the rolling effectiveness of the ailerons by inducing sideslip – particularly in the high–lift–coefficient range. In some instances, a sizeable deflection of the rudder may be required to perform a coordinated roll. It is well to note, however, that these adverse yawing moments are comparable to those produced by conventional flap–type ailerons (reference 17).

CONCLUSIONS

An investigation of triangular– and parallelogram–plan–form deflectable wing–tip ailerons on an untapered 45° sweptback semispan wing with and without an end plate (simulating a vertical fin) was performed in the Langley 300 MPH 7– by 10–foot tunnel. The rectangular end plate was mounted on the wing just inboard of the ailerons. The results of the investigation led to the following conclusions:

1. Each of the aileron configurations investigated should provide adequate lateral control over the entire angle–of–attack range investigated.

2. The yawing moments resulting from aileron deflection were generally adverse – particularly at large angles of attack and aileron deflections.

3. Adding the end plate to the wing increased the wing lift-curve slope and the drag, but decreased the wing maximum lift and the lift-drag ratios appreciably and also decreased the aileron effectiveness.

4. Aileron plan form generally had little effect on the values of rolling-moment coefficient and yawing-moment coefficient produced by aileron deflection, or on the lift, drag, and pitching-moment characteristics of the wing model.

Langley Aeronautical Laboratory
National Advisory Committee for Aeronautics
Langley Air Force Base, Va.

REFERENCES

1. Knight, Montgomery, and Bamber, Millard J.: Wind Tunnel Tests on a Model of a Monoplane Wing with Floating Ailerons. NACA TN 316, 1929.

2. Weick, Fred E., and Harris, Thomas A.: Wind-Tunnel Research Comparing Lateral Control Devices, Particularly at High Angles of Attack. IV - Floating Tip Ailerons on Rectangular Wings. NACA Rep. 424, 1932.

3. Weick, Fred E., and Harris, Thomas A.: Wind-Tunnel Research Comparing Lateral Control Devices, Particularly at High Angles of Attack. XI. Various Floating Tip Ailerons on Both Rectangular and Tapered Wings. NACA TN 458, 1933.

4. Soulé, H. A., and Gracey, W.: A Flight Comparison of Conventional Ailerons on a Rectangular Wing and of Conventional and Floating Wing-Tip Ailerons on a Tapered Wing. NACA Rep. 630, 1938.

5. Turner, Thomas R., Lockwood, Vernard E., and Vogler, Raymond D.: Preliminary Investigation of Various Ailerons on a 42° Sweptback Wing for Lateral Control at Transonic Speeds. NACA RM L8D21, 1948.

6. Hagerman, John R., and O'Hare, William M.: Investigation of Extensible Wing-Tip Ailerons on an Untapered Semispan Wing at 0° and 45° Sweepback. NACA RM L9H04, 1949.

7. Polhamus, Edward C.: Jet-Boundary-Induced-Upwash Velocities for Swept Reflection-Plane Models Mounted Vertically in 7- by 10-Foot, Closed, Rectangular Wind Tunnels. NACA TN 1752, 1948.

8. Herriot, John G.: Blockage Corrections for Three-Dimensional-Flow Closed-Throat Wind Tunnels, with Consideration of the Effect of Compressibility. NACA RM A7B28, 1947.

9. Swanson, Robert S., and Toll, Thomas A.: Jet-Boundary Corrections for Reflection-Plane Models in Rectangular Wind Tunnels. NACA Rep. 770, 1943.

10. Bates, William R.: Collection and Analysis of Wind-Tunnel Data on the Characteristics of Isolated Tail Surfaces with and without End Plates. NACA TN 1291, 1947.

11. Hemke, Paul E.: Drag of Wings with End Plates. NACA Rep. 267, 1927.

12. Polhamus, Edward C.: A Simple Method of Estimating the Subsonic Lift and Damping in Roll of Sweptback Wings. NACA TN 1862, 1949.

13. Lange and Wacke: Test Report on Three- and Six-Component Measurements on a Series of Tapered Wings of Small Aspect Ratio (Partial Report: Triangular Wing). NACA TM 1176, 1948.

14. Winter, H.: Flow Phenomena on Plates and Airfoils of Short Span. NACA TM 798, 1936.

15. Goodman, Alex, and Adair, Glenn H.: Estimation of the Damping in Roll of Wings through the Normal Flight Range of Lift Coefficient. NACA TN 1924, 1949.

16. Anon: U. S. Air Force Specification for Flying Qualities of Piloted Airplanes. No. 1815-B, June 1948.

17. Fischel, Jack, and Schneiter, Leslie E.: An Investigation at Low Speed of a 51.3° Sweptback Semispan Wing Equipped with 16.7-Percent-Chord Plain Flaps and Ailerons Having Various Spans and Three Trailing-Edge Angles. NACA RM L8H20, 1948.

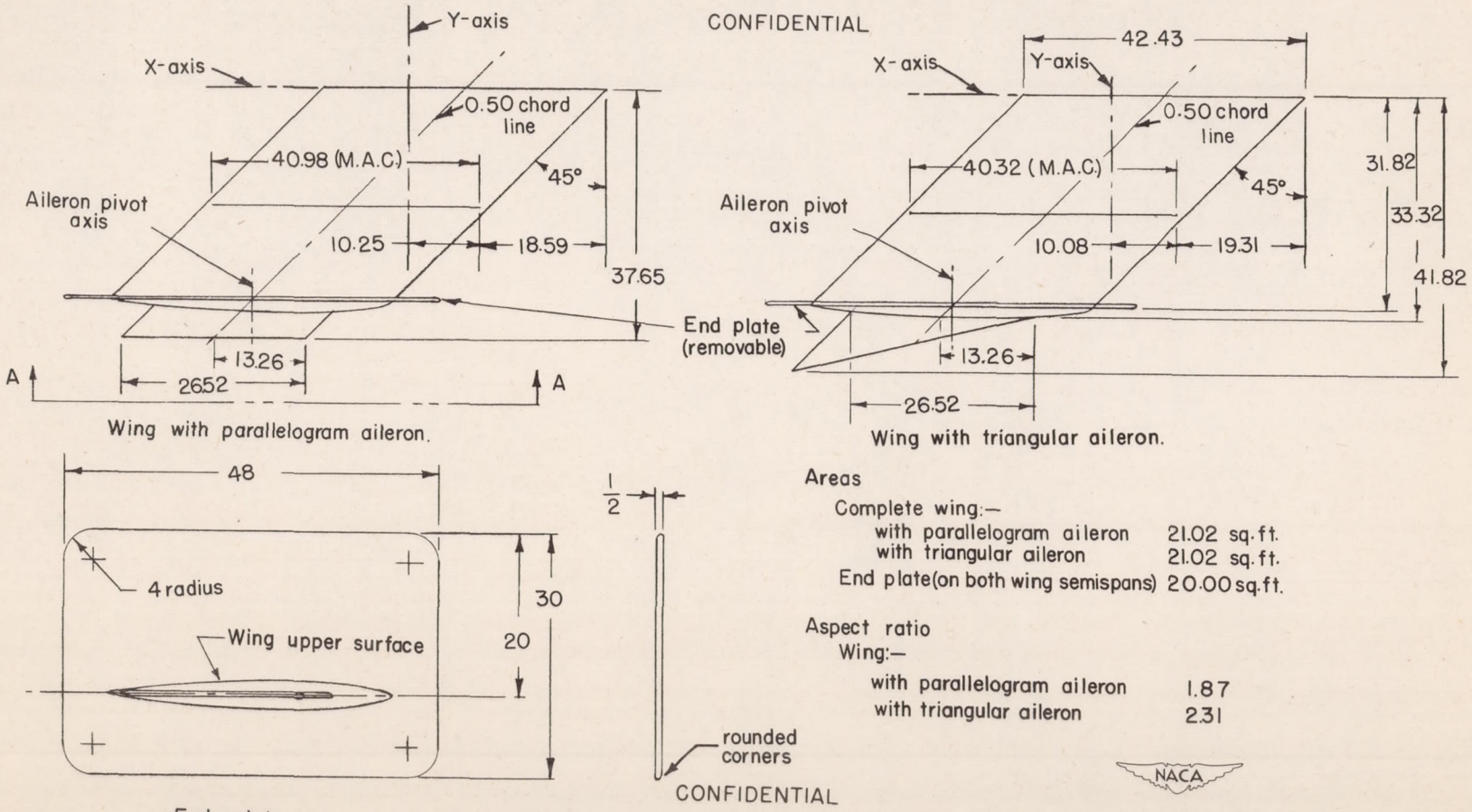

Areas

Complete wing:—

with parallelogram aileron	21.02 sq. ft.
with triangular aileron	21.02 sq. ft.
End plate (on both wing semispans)	20.00 sq. ft.

Aspect ratio

Wing:—

with parallelogram aileron	1.87
with triangular aileron	2.31

Figure 1.— Geometric characteristics of the 45° sweptback wing, wing-tip ailerons, and end plate. (All dimensions in inches unless otherwise noted.)

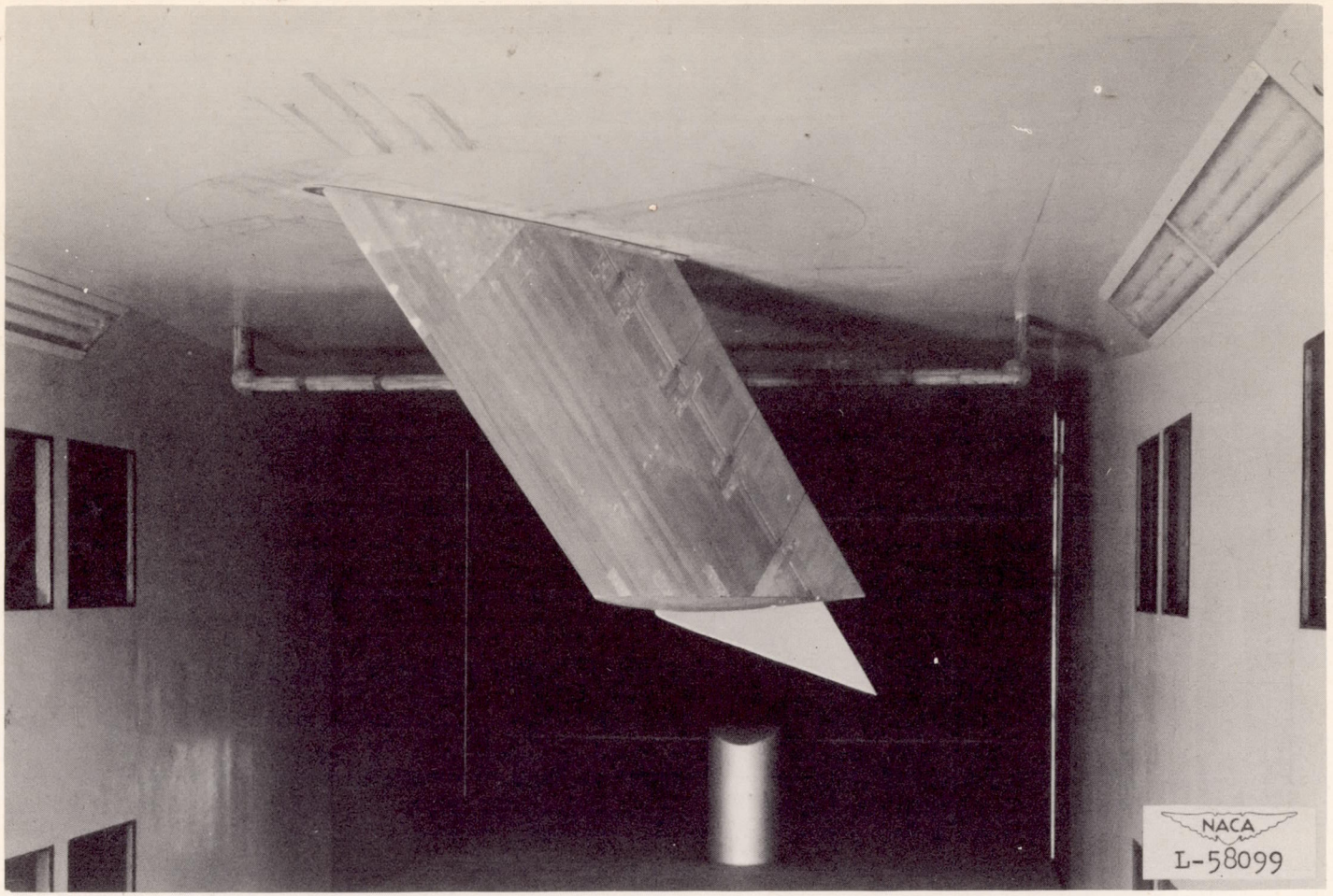

Figure 2.– The 45° sweptback semispan wing mounted in the Langley 300 MPH 7– by 10–foot tunnel. Plain wing with triangular wing–tip aileron.

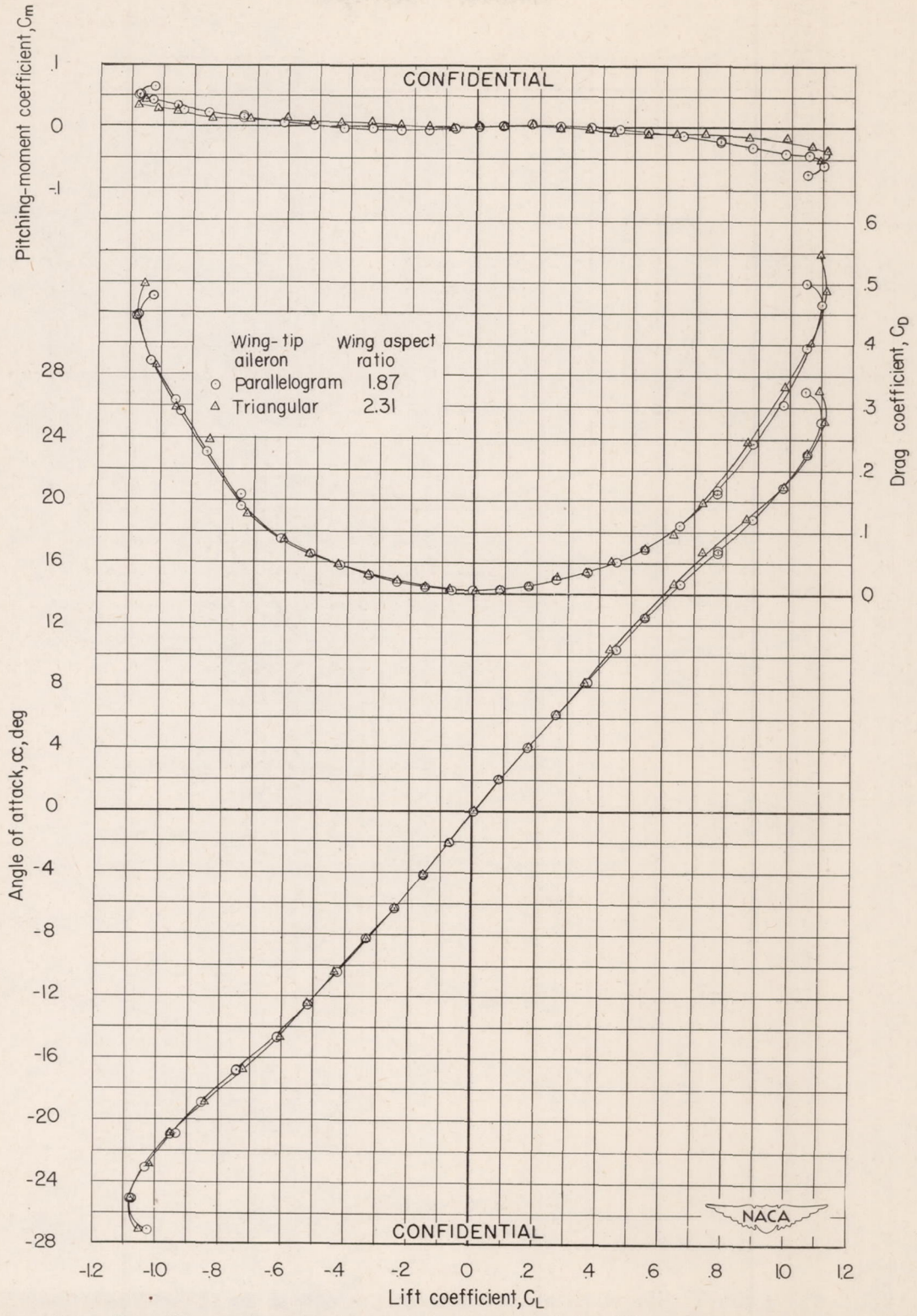

Figure 3.— The aerodynamic characteristics in pitch of the 45° sweptback wing equipped with deflectable wing-tip ailerons. Plain wing. $\delta_a = 0°$

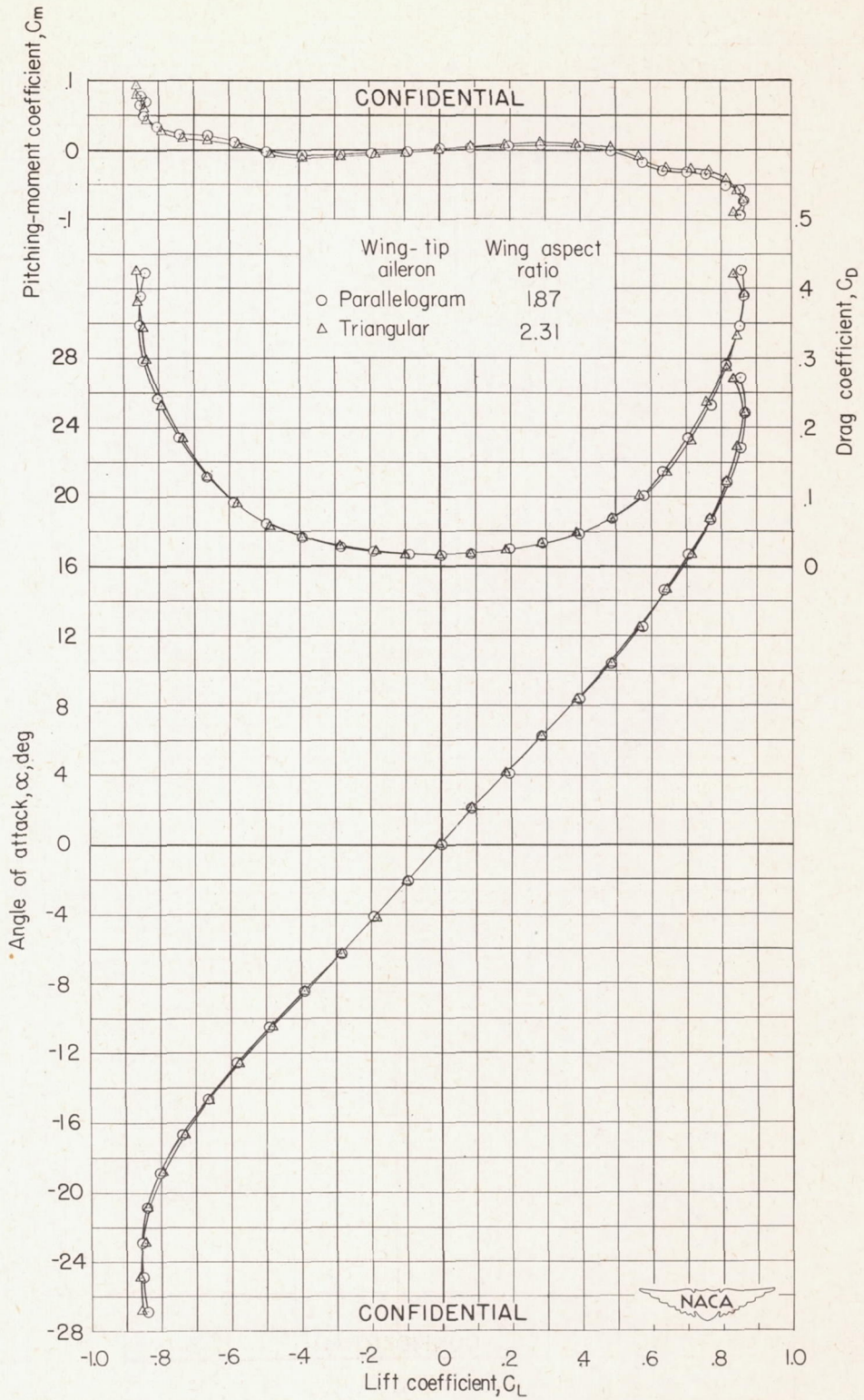

Figure 4. — The aerodynamic characteristics in pitch of the 45° sweptback wing equipped with deflectable wing-tip ailerons. Wing with end plate; $\delta_a = 0°$.

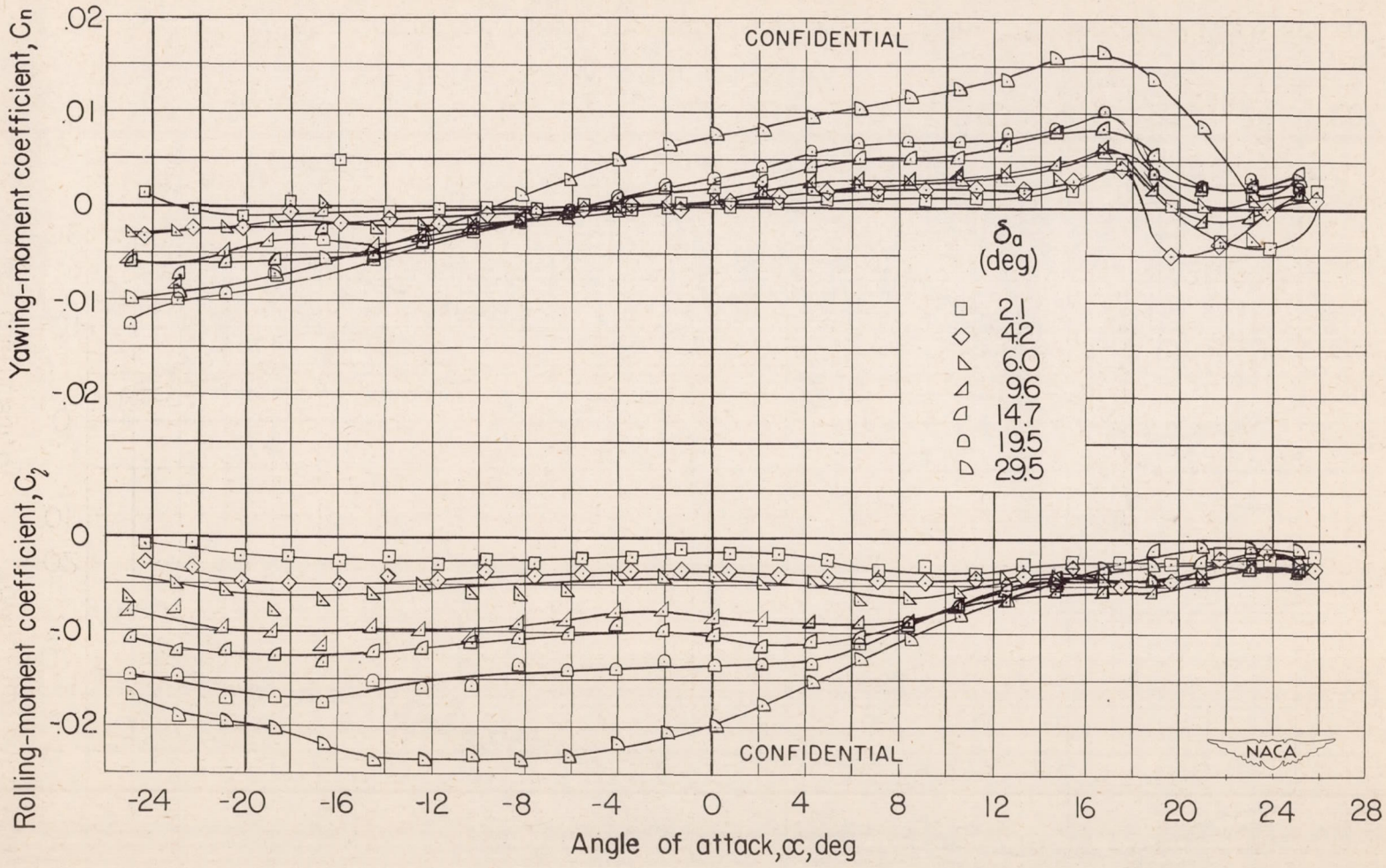

Figure 5.— The rolling-moment and yawing-moment characteristics of the 45° sweptback wing for various deflections of the triangular wing-tip aileron. Plain wing.

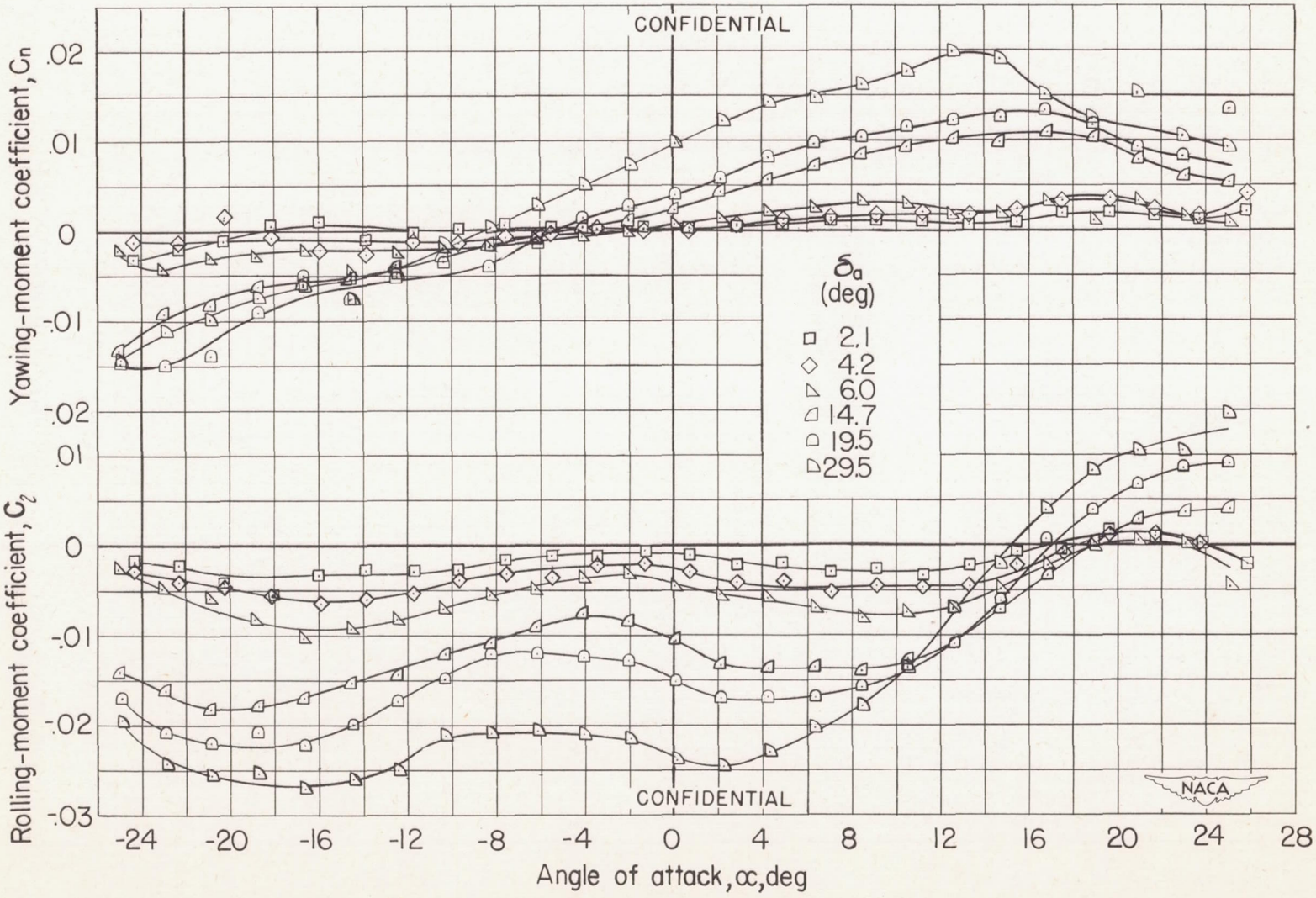

Figure 6.— The rolling-moment and yawing-moment characteristics of the 45° sweptback wing for various deflections of the parallelogram wing-tip aileron. Plain wing.

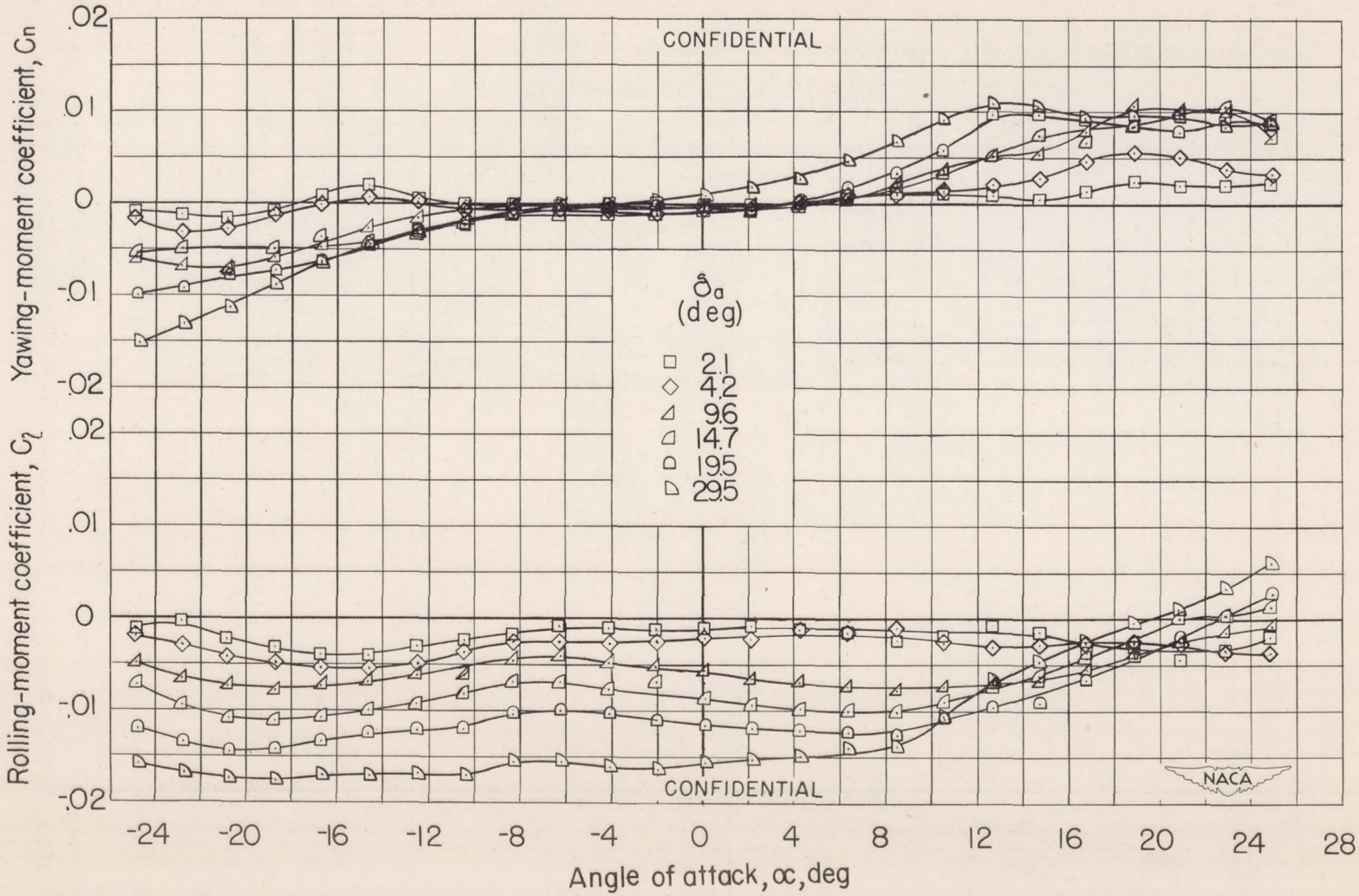

Figure 7.— The rolling-moment and yawing-moment characteristics of the 45° sweptback wing for various deflections of the triangular wing-tip aileron. Wing with end plate.

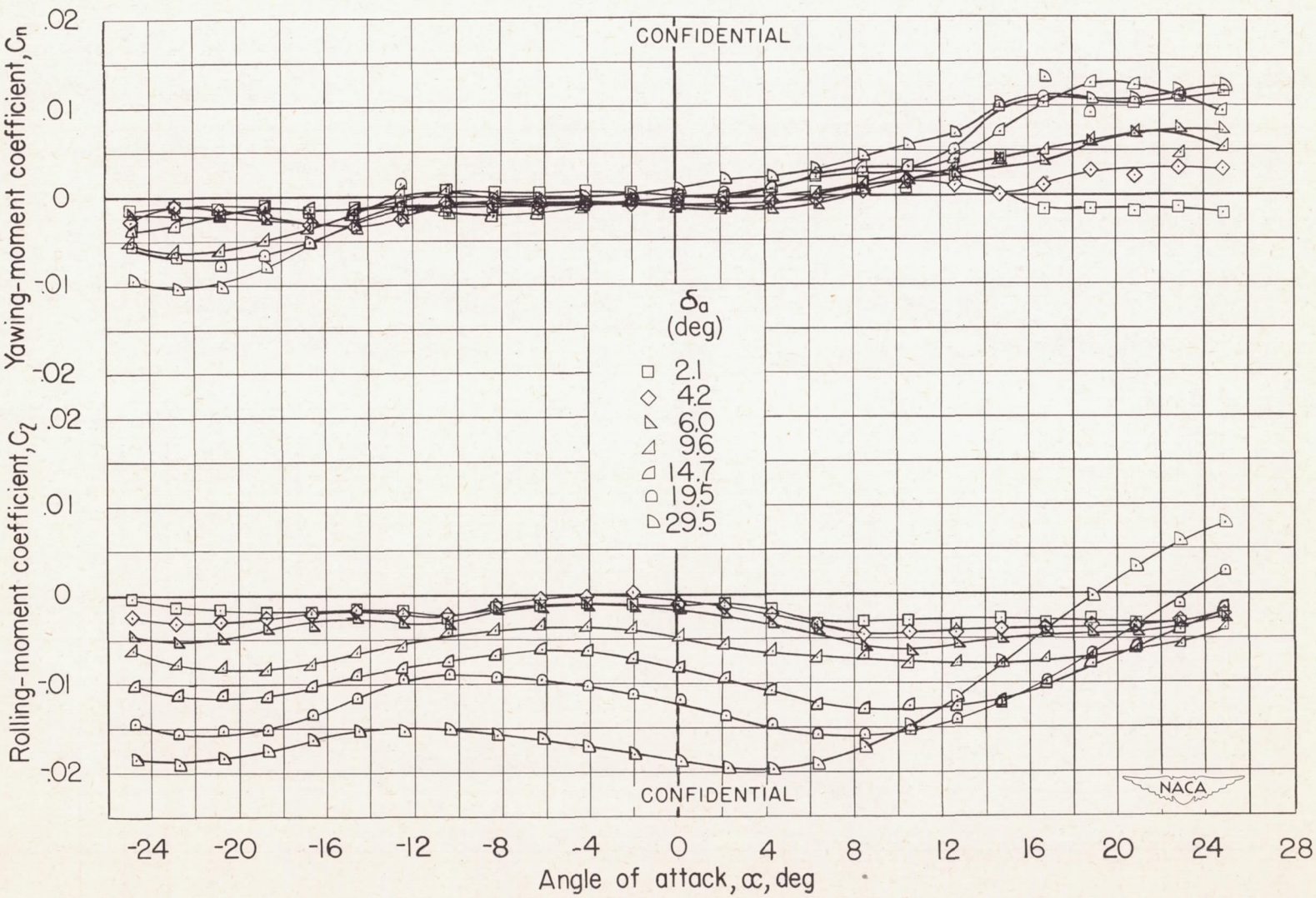

Figure 8. — The rolling-moment and yawing-moment characteristics of the 45° sweptback wing for various deflections of the parallelogram wing-tip aileron. Wing with end plate.

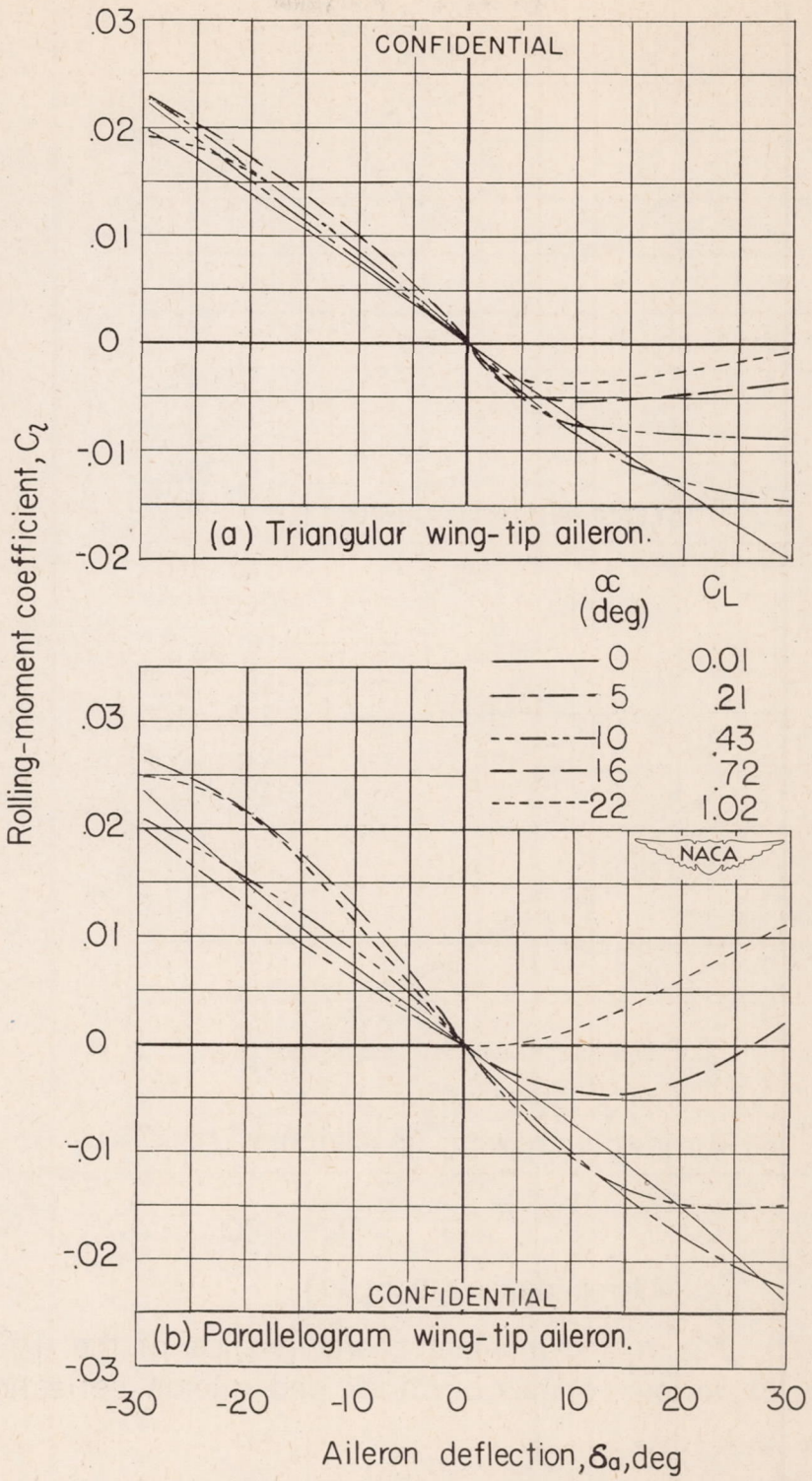

Figure 9.— The rolling-moment characteristics of the 45° sweptback wing at various angles of attack and aileron deflections. Plain wing.

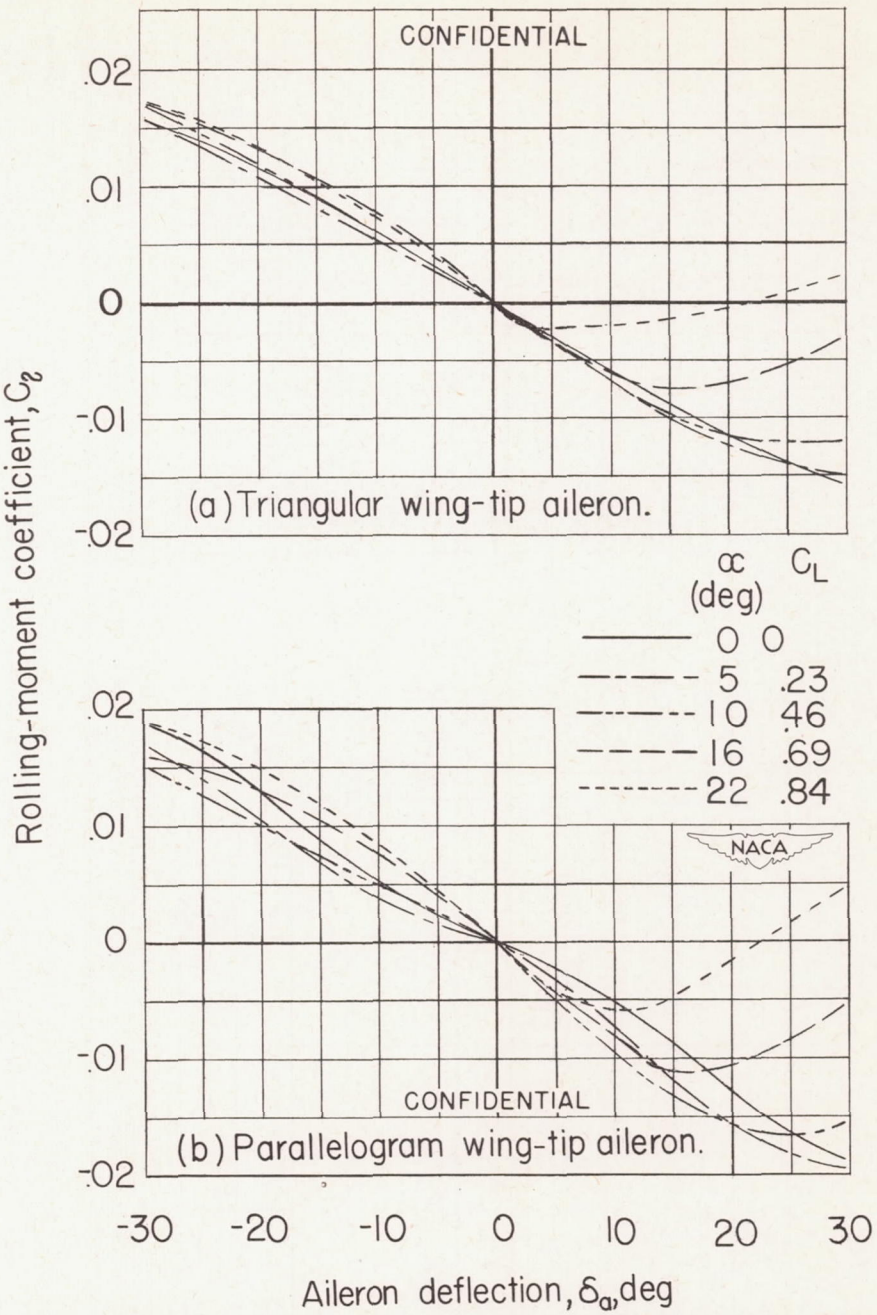

Figure 10.— The rolling-moment characteristics of the 45° sweptback wing at various angles of attack and aileron deflections. Wing with end plate.

CONFIDENTIAL

⊙ Triangular aileron
△ Parallelogram aileron } Present investigation
⊡ Triangular tip aileron on wing of reference 5 (Mach number=0.5)

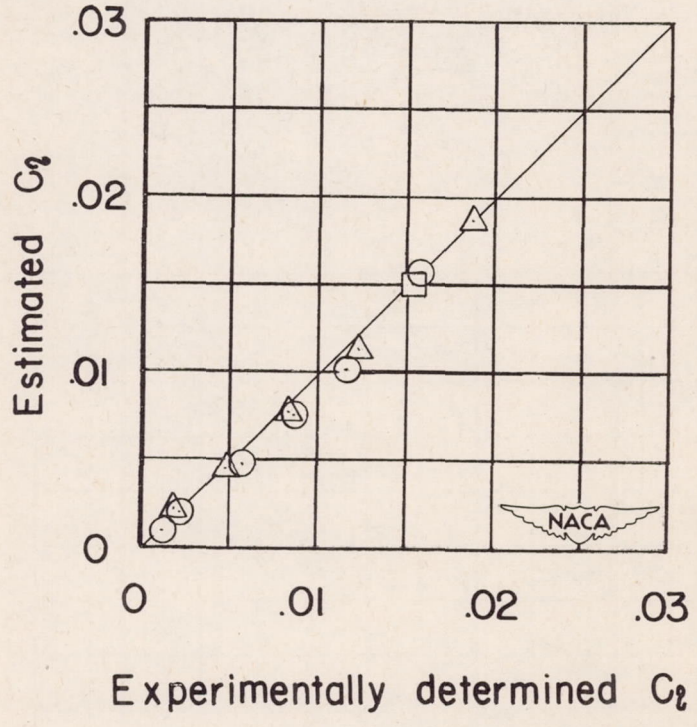

CONFIDENTIAL

Figure 11.— Comparison of experimentally determined values of C_ℓ with estimated values of C_ℓ for deflectable wing-tip ailerons in the presence of an end plate. $\alpha = 0°$.

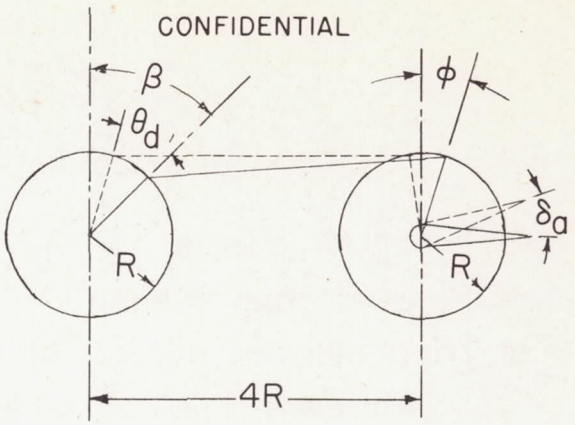

	Differential	$\delta_{a_{max}}$	β	ϕ
—— ——	1:1	29.5°,-29.5°	0°	0°
- - - - - -	2:1	15.5°,-29.5°	40°	6.9°
———	3:1	11.2°,-29.5°	47°	11.8°

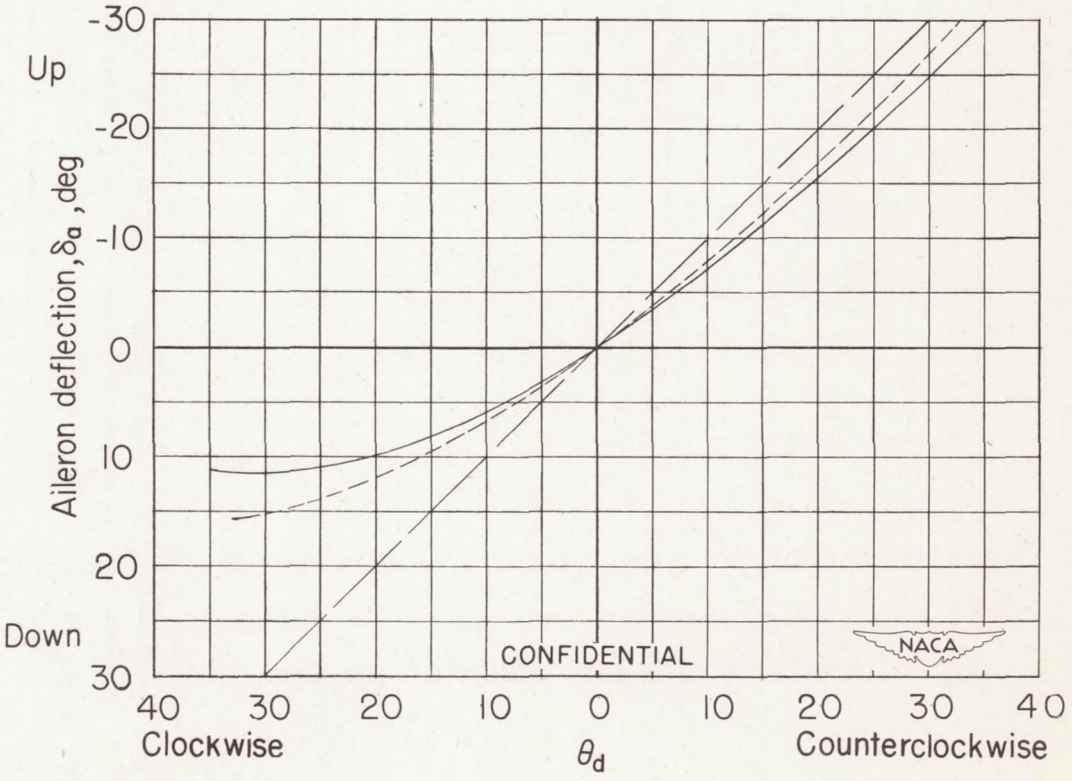

Figure 12.— Differential linkage systems used for determining $\frac{pb}{2V}$.

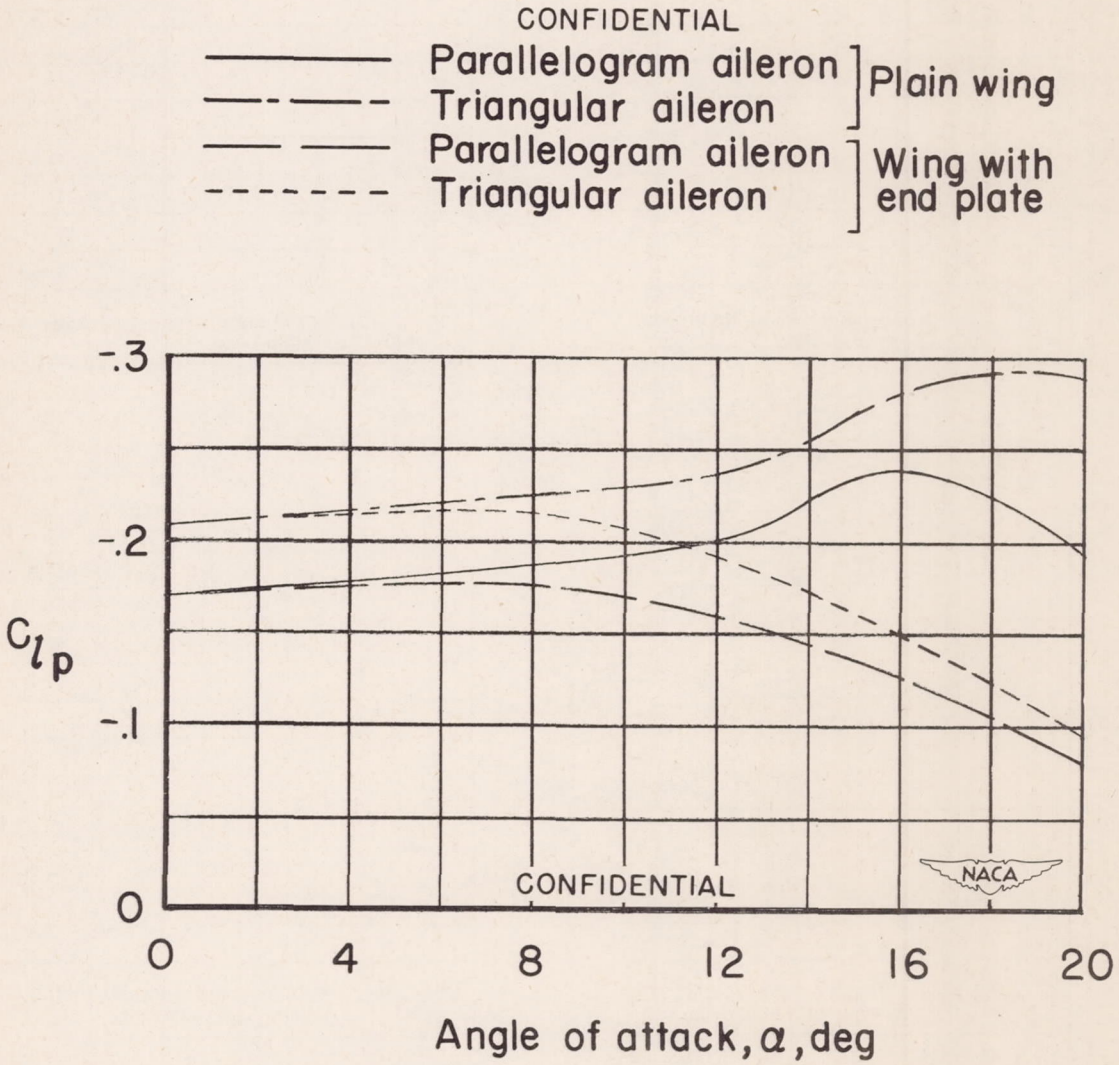

Figure 13.— Variation of C_{l_p} (used for determining $\frac{pb}{2V}$) with angle of attack.

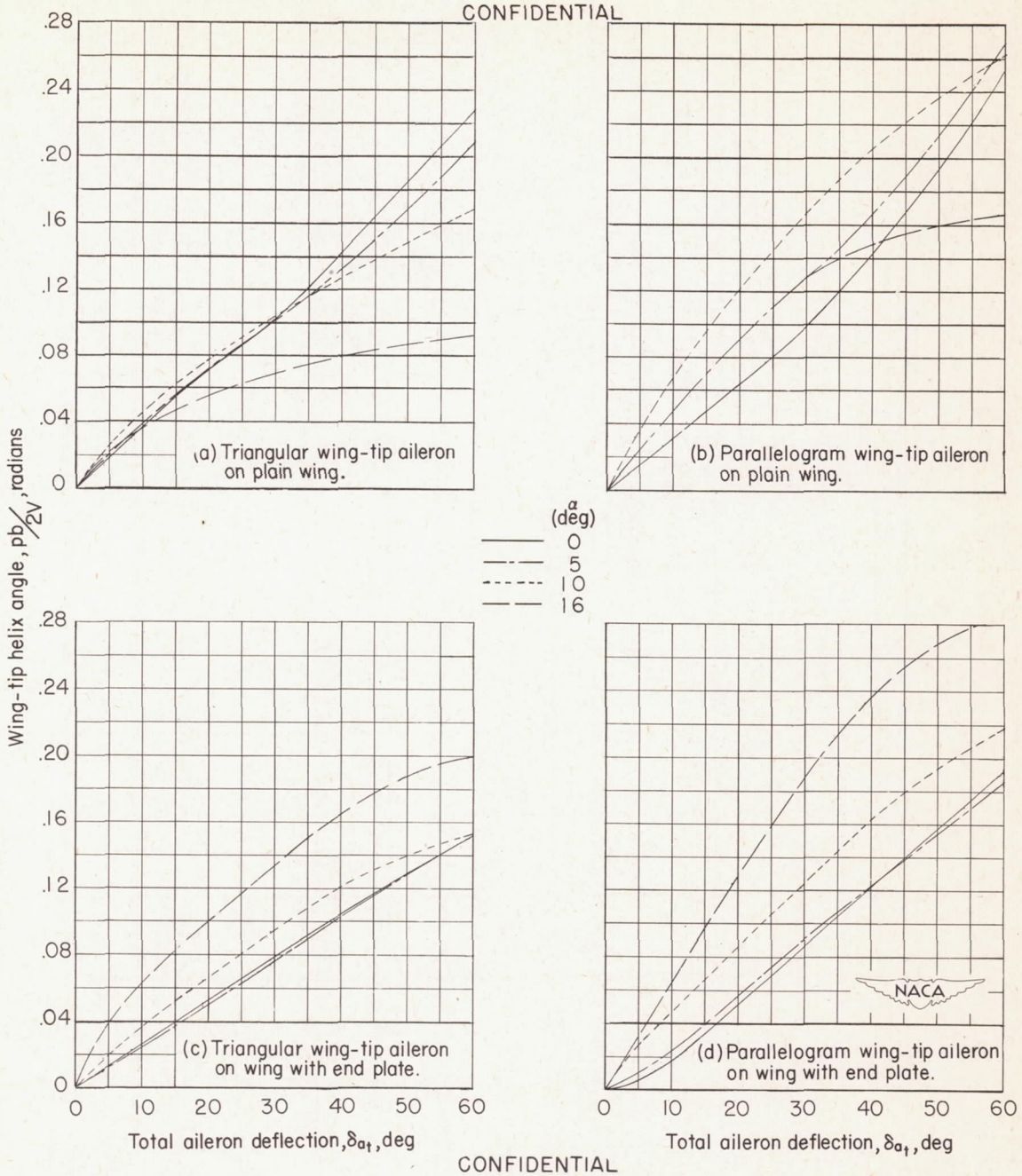

Figure 14.— Variation of estimated wing-tip helix angle $\frac{pb}{2V}$ with total aileron deflection for the 45° sweptback complete wing. Aileron differential, 1:1.

CONFIDENTIAL

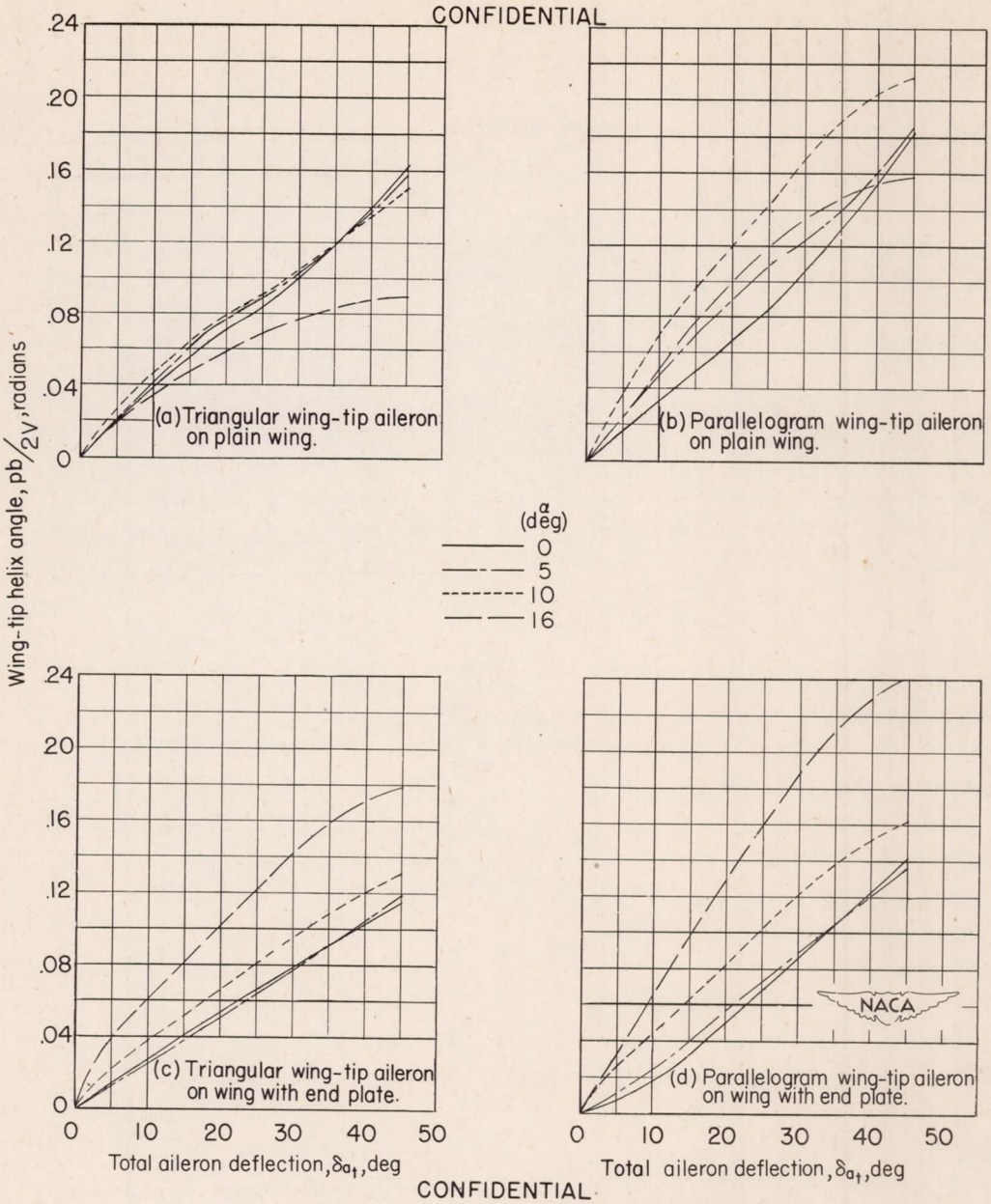

CONFIDENTIAL

Figure 15.—Variation of estimated wing-tip helix angle $\frac{pb}{2V}$ with total aileron deflection for the 45° sweptback complete wing. Aileron differential, 2:1 (approximately).

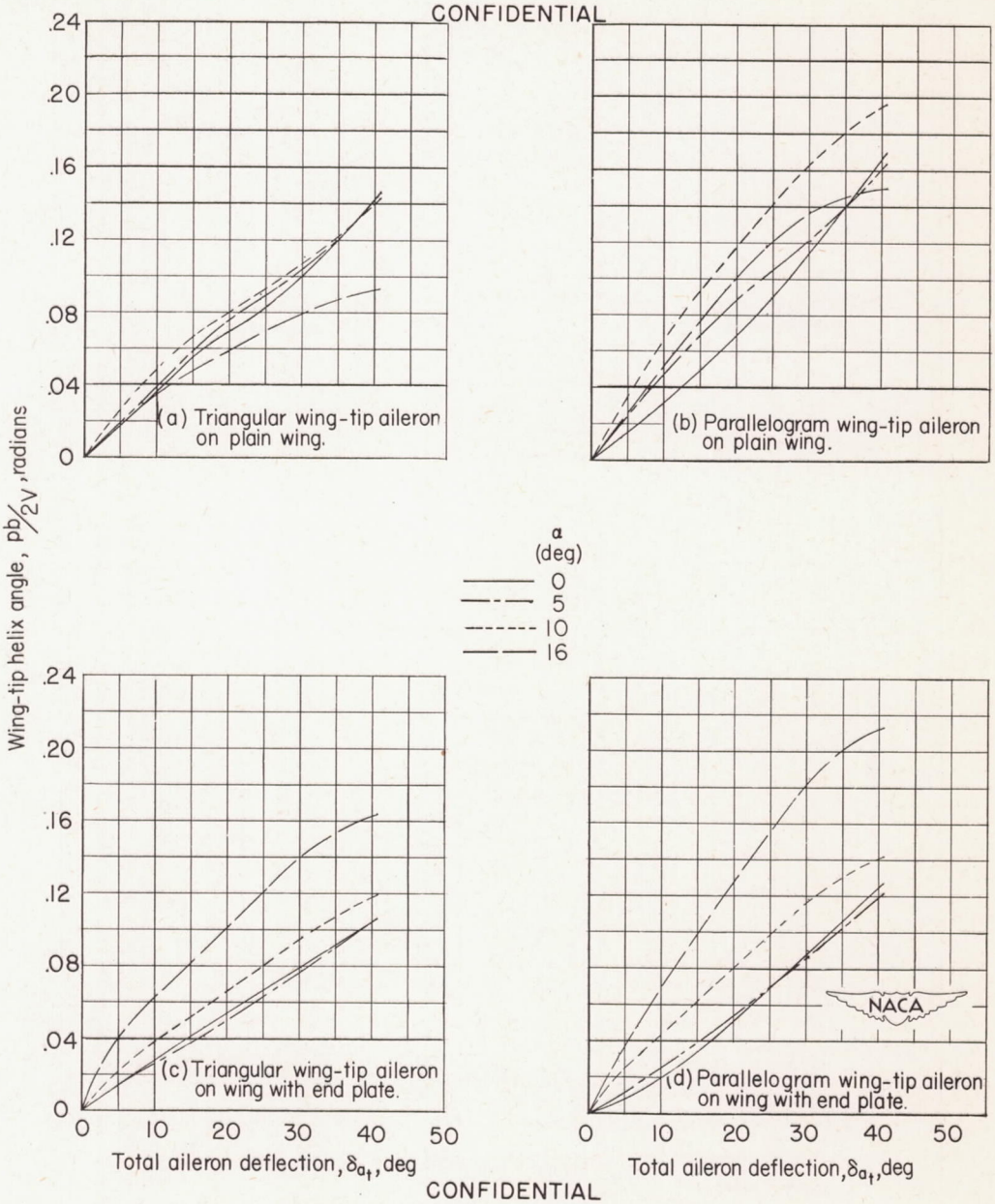

Figure 16.—Variation of estimated wing-tip helix angle $\frac{pb}{2V}$ with total aileron deflection for the 45° sweptback complete wing. Aileron differential, 3:1 (approximately).